ACS APPLIED MATERIALS & INTERFACES

Research Article

www.acsami.org

Junctionless Diode Enabled by Self-Bias Effect of Ion Gel in Single-Layer MoS_2 Device

Muhammad Atif Khan,[†] Servin Rathi,[†] Jinwoo Park,[†] Dongsuk Lim,[†] Yoontae Lee,[†] Sun Jin Yun,[‡] Doo-Hyeb Youn,[‡] and Gil-Ho Kim*[,†]

[†]School of Electronic and Electrical Engineering and Sungkyunkwan Advanced Institute of Nanotechnology (SAINT), Sungkyunkwan University, Suwon 16419, South Korea

[‡]ICT Components and Materials Technology Research Division, Electronics and Telecommunications Research Institute, Daejeon 34129, Republic of Korea

Supporting Information

ABSTRACT: The self-biasing effects of ion gel from source and drain electrodes on electrical characteristics of single layer and few layer molybdenum disulfide (MoS_2) field-effect transistor (FET) have been studied. The self-biasing effect of ion gel is tested for two different configurations, covered and open, where ion gel is in contact with either one or both, source and drain electrodes, respectively. In open configuration, the linear output characteristics of the pristine device becomes nonlinear and on−off ratio drops by 3 orders of magnitude due to the increase in "off" current for both single and few layer MoS_2 FETs. However, the covered configuration results in a highly asymmetric output characteristics with a rectification of around 10^3 and an ideality factor of 1.9. This diode like behavior has been attributed to the reduction of Schottky barrier width by the electric field of self-biased ion gel, which enables an efficient injection of electrons by tunneling at metal-MoS_2 interface. Finally, finite element method based simulations are carried out and the simulated results matches well in principle with the experimental analysis. These self-biased diodes can perform a crucial role in the development of high-frequency optoelectronic and valleytronic devices.

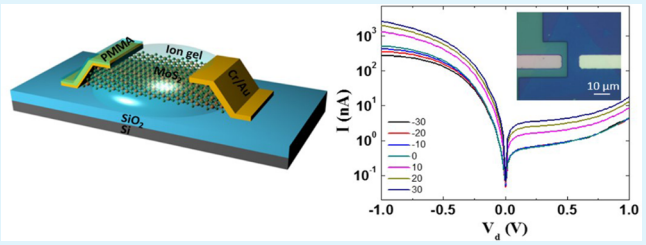

KEYWORDS: *ion gel, molybdenum disulfide, diode, self-biasing, Silvaco*

1. INTRODUCTION

Transition metal dichalcogenides (TMDs) have attracted great interest for postsilicon electronics because of their unique properties like atomic thickness and sizable band gap. Moreover, their high optical absorption and mechanical flexibility make them a strong candidate for optoelectronics and photovoltaic applications.[1−3] Currently, most of the TMDs based devices use oxide gate dielectric layers to switch the device between on and off state.[4−6] However, large operating voltage window of oxide gate for highly doped channel can be overcome by using an electrolyte that forms electric double-layer (EDL) capacitors under applied bias. This robust channel charge modulation capacity of EDLs is because of their high specific capacitance of around 1 μF cm^{-2}, which allows the depletion mode devices to operate at significantly reduced voltage. Moreover, these electrolytes are solution process able and compared to oxides, their processing temperatures are also much lower, which makes them highly suitable for flexible electronics.[7−11] Besides their applications in organic electronics, EDLs, commonly referred as ion gel, have also been frequently used in TMDs based devices to achieve ambipolar operation, superconductivity and for demonstrating proof-of-the-concept electronic devices.[12,13] Devices based on layered materials like MoS_2, WSe_2, $SnSe_2$, graphene, and WS_2 have been studied using ion gel as gate dielectric.[14−17] Moreover, p−n junction has also been fabricated in a single flake of MoS_2 using ion freezing technique under a constant bias at low temperature.[18] In this work, we have studied the self-biasing effect of ion gel from source and drain electrodes on the electrical properties of MoS_2 field effect transistor (FET). We have also demonstrated the operation of self-biased diodes by using asymmetric biasing technique where one electrode bias the ion-gel while the other electrode is passivized with poly(methyl methacrylate) (PMMA) in a two probe FET configuration. This resulted in an extreme asymmetry in $I-V_d$ curve with a rectification ratio of around 10^3. In conventional design, the rectification in a p−n junction is usually achieved by controlled doping of semiconductor, however, conventional doping techniques like ion-implantation, thermal diffusion, etc., have limitations at ultrasmall channels.[19,20] Therefore, the proposed self-biased diode can be a promising candidate at this scale since it does not require conventional doping of semiconductor. Furthermore, the transparent nature of the top gate dielectric (ion gel)

Received: May 1, 2017
Accepted: July 17, 2017
Published: July 17, 2017

DOI: 10.1021/acsami.7b06071
ACS Appl. Mater. Interfaces 2017, 9, 26983−26989

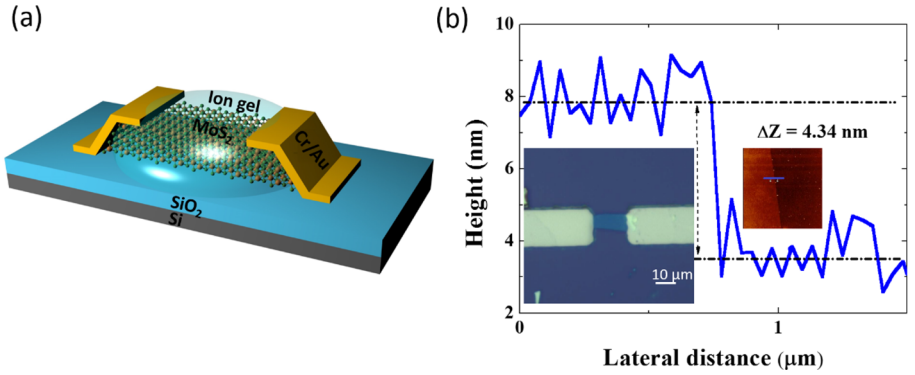

Figure 1. (a) Schematic of multilayer MoS_2 FET covered with ion gel. (b) Atomic force microscopy (AFM) image of six layer MoS_2 with height profile (inset shows the optical microscope image of the device).

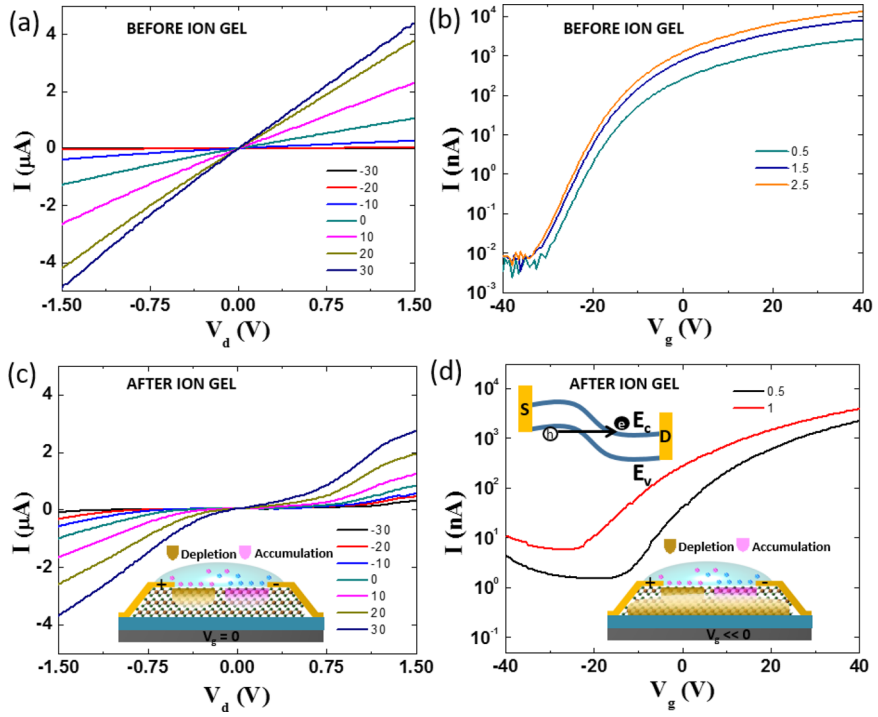

Figure 2. (a) Output curve of pristine six layers MoS_2 FET at different back gate voltages. (b) Transfer curve of pristine six layers MoS_2 FET at different drain voltages. (c) Output curve of six layers MoS_2 FET at different back gate voltages after introduction of ion gel. (d) Transfer curve of six layers MoS_2 FET at different drain voltages after introduction of ion gel.

makes it suitable for optoelectronics and photovoltaic applications.

Figure 1a and b show the schematic and optical image of the multilayer MoS_2 FET used in the experiment. The thickness of multilayer MoS_2 was 4.34 nm (6 layers), as determined by atomic force microscopy and shown in Figure 1b. Besides the study of multilayer MoS_2, single-layer MoS_2 based devices were also studied and the thickness was confirmed by Raman spectroscopy (Figure S1) where the difference in frequencies of E_{2g}^1 and A_{1g} peak, 18 cm^{-1}, confirms that the MoS_2 flake is single layer.[21] The electrical characteristics of multilayer MoS_2 FET are discussed first. All the electrical measurements are performed at room temperature under vacuum conditions using Keithley 4200 semiconductor characterization system (4200-SCS).

2. RESULTS AND DISCUSSION

Figure 2 illustrates the electrical characteristics of multilayer MoS_2 FET before and after the introduction of ion gel. For the device with ion gel, a droplet of ionic liquid was dropped using micropipette to immerse channel as well as source and drain electrodes as shown in Figure 1a. Figure 2a shows the output characteristics of the pristine device at different back gate voltages. The linear $I-V_d$ curve indicates the formation of Ohmic contacts between contact metal and MoS_2. In Figure 2b, the transfer characteristics shows good current modulation and a high on/off ratio of $\sim 10^6$, when the back gate voltage is swept from −40 to 40 V. After the electrical measurement of the pristine device, ion gel was introduced and the output and transfer characteristics were measured again. Figure 2c shows the output characteristics of the device with ion gel, although the drain current remained almost same but the $I-V_d$ curve become nonlinear. This transition from linear to nonlinear behavior can be explained by considering the field effect of the

DOI: 10.1021/acsami.7b06071
ACS Appl. Mater. Interfaces 2017, 9, 26983−26989

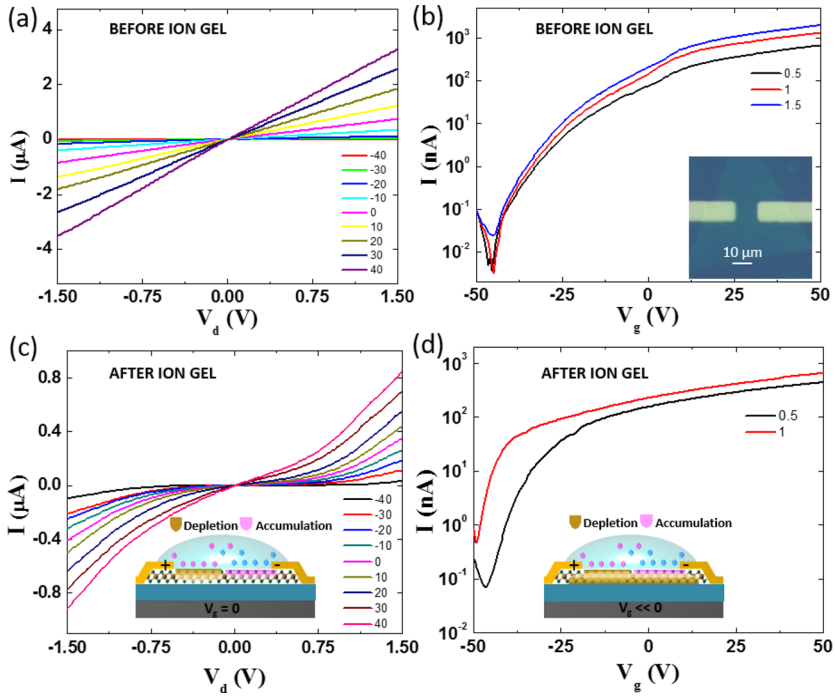

Figure 3. (a) Output curve of pristine single layers MoS_2 FET at different back gate voltages. (b) Transfer curve of pristine single layers MoS_2 FET at different drain voltages (inset shows the optical microscope image of device). (c) Output curve of single layers MoS_2 FET at different back gate voltages after introduction of ion gel. (d) Transfer curve of single layers MoS_2 FET at different drain voltages after introduction of ion gel.

ion gel on the MoS_2 channel in the vicinity of source and drain electrodes as illustrated in inset of Figure 2c.

The channel in the vicinity of the negative electrode will accumulate electrons induced by the positive electric field generated by the polarized ions from the ion gel. This separation of positive ions is due to biasing of the ion gel from the negative electrode. Similarly, the channel in the vicinity of the positive electrode is depleted of electrons because of the negative electric field from the ion gel. The modulating electric field near the electrodes is generated by the accumulation of opposite polarity ions which are induced by the applied voltage at the electrodes, as explained by schematic in Figure 2c.[11,18] Because of this opposite ion gel gating effect at the electrodes, the total current through the device remains essentially same. Since the behavior is symmetric for positive and negative polarities, in Figure 2d, we show back gate voltage sweep for only positive drain bias. Figure 2d is the transfer curve of device after introduction of ion gel and an on/off ratio of $\sim 10^3$ can be seen in drain current, when the back gate voltage is swept from −40 to 40 V. After the introduction of ion gel, the "off" current is increased from 10 pA (Figure 2b) to around 10 nA at $V_d = 1$ (Figure 2d), which results in the on/off ratio decreasing from $\sim 10^6$ to 10^3. This can be explained by combining the field effects of ion gel and back gate. As shown in inset of Figure 2d, at negative back gate bias, the negative electric field starts depleting the accumulated electrons in the entire channel. Similarly, positive electrode is also depleting the electrons in its vicinity by the virtue of negative electric field from the ion gel. On the contrary, the positive electric field at the negative electrode accumulates electrons in the MoS_2 channel. In the positive gate bias regime, these accumulated electrons do not play a significant role because of the similar order concentration of the background carriers in the channel, however they start affecting the device characteristics in the negative back gate bias regime where the contribution of the ion gel induced electrons (near negative electrode) to total current becomes significant and can be seen as increase in "off" current. Although the "on" current remains essentially unchanged for all drain bias, yet the "off" current increases from 5 to 10 nA, when the drain bias is increased from 0.5 to 1 V, respectively. This is in contrast to the constant "off" current (at −40 V back gate voltage) observed in the pristine device, when the drain voltage is varied from 0.5 to 2.5 V (Figure 2b). Another reason for increase in "off" current can be gate induced drain leakage current (GIDL). In the presence of high electric field from back gate as well as ion gel, the valence band and conduction band will align as shown in inset of Figure 2d. This alignment will assist tunneling of electrons directly from valence to conduction band and results in generation of electron−hole pairs. These electrons-holes pairs can flow toward electrodes and result in an increased leakage current. This effect of ion gel on the "off" current gives an important insight into the working of ion gel FETs where the impact of applied drain voltage on the device characteristics can be overcome by electrically isolating the electrodes.

Next we investigate the electrical characteristics of single layer MoS_2 with ion gel as shown in Figure 3. The linear $I-V_d$ curves show Ohmic contacts before introduction of ion gel as shown in Figure 3a. After the introduction of ion gel, the $I-V_d$ curves become nonlinear but remained symmetrical for positive and negative voltages, which can be attributed to the local biasing effect of ion gel at both electrodes as shown in inset of Figure 3c. Although drain current remained same in the ion gel multilayer MoS_2 device but after the introduction of ion gel to the single layer device, the drain current decreases around four times as compared to the pristine device. This reduction in current in the single layer device can be attributed to a combination of several factors like higher band gap, different dielectric and screening environment to the carriers as compared to the multilayer device. As in multilayer MoS_2 device, the majority of current flows in middle layers,[22]

DOI: 10.1021/acsami.7b06071
ACS Appl. Mater. Interfaces 2017, 9, 26983−26989

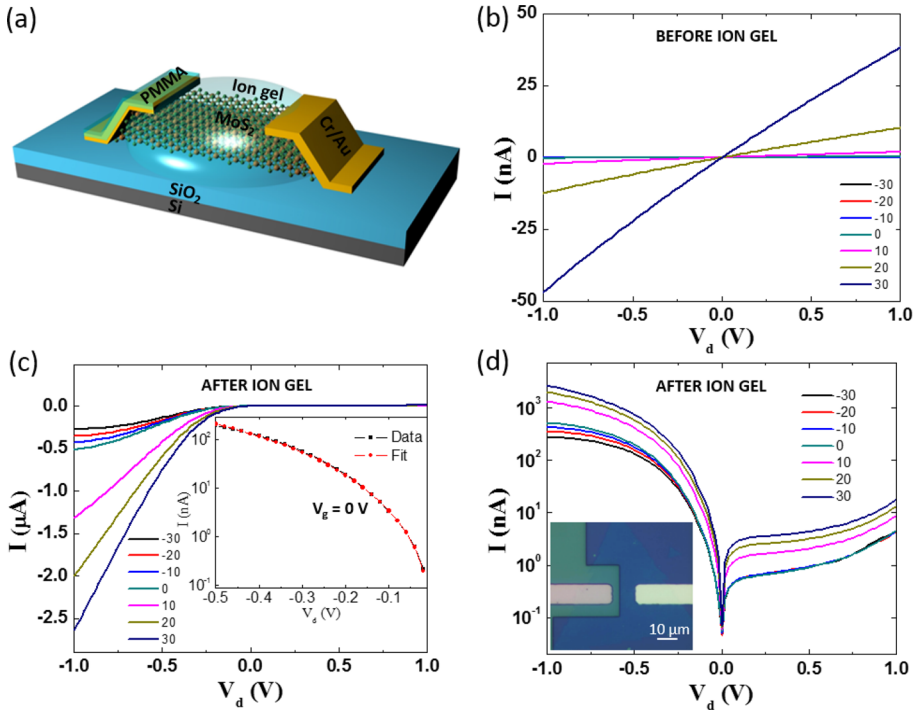

Figure 4. (a) Schematic of self-biased single layer MoS_2 FET covered with ion gel with one contact encapsulated by PMMA. (b) Plot of drain current and drain voltage at different back gate voltages of single layers MoS_2 FET before introduction of gel. (c) Plot of drain current and drain voltage at different back gate voltages of single layers MoS_2 FET after introduction of gel in linear scale (inset shows the fitting of data in diode equation with an ideality factor of 1.9). (d) Plot of panel c in semilog scale (inset shows the optical microscope image of device).

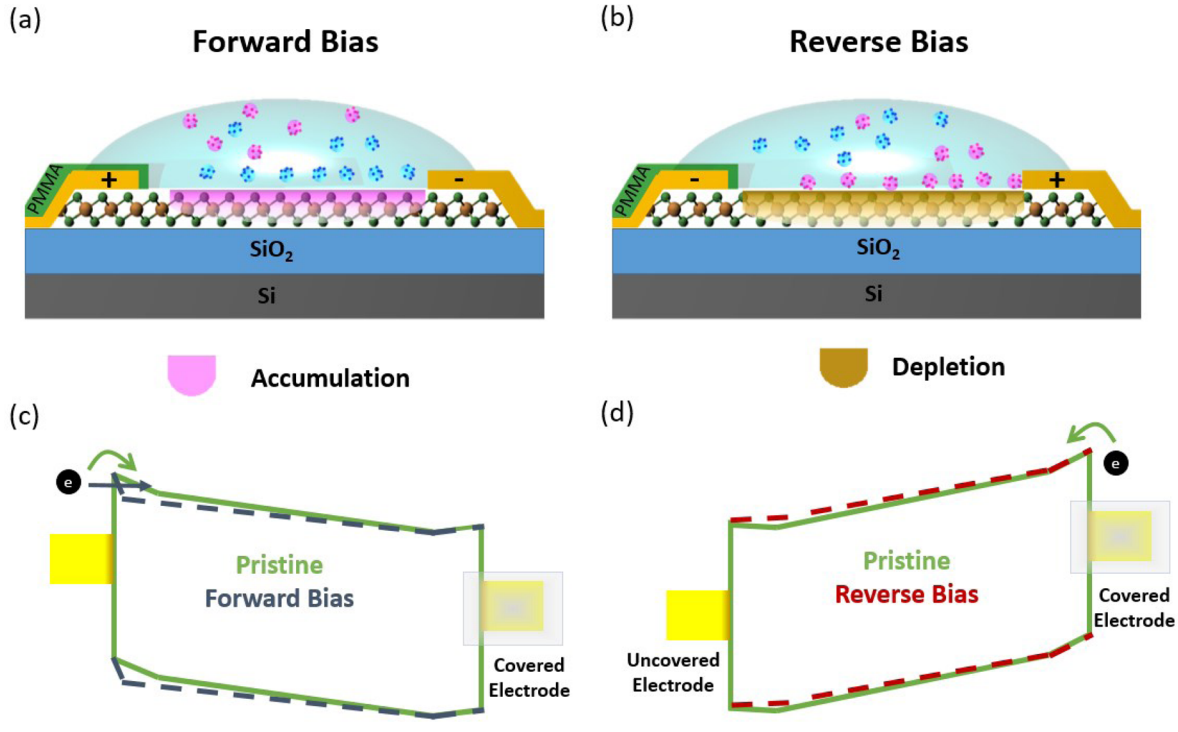

Figure 5. (a) Schematic showing accumulation of electrons in self-biased MoS_2 diode under forward bias. (b) Schematic showing depletion of electrons in self-biased MoS_2 diode under reverse bias. (c) Schematic band structure of pristine MoS_2 FET and self-biased diode during forward bias. (d) Schematic band structure of pristine MoS_2 FET and self-biased diode during reverse bias.

therefore, introduction of a new interface such as ion gel does not have a significant effect on current because of the dielectric encapsulation and screening of charge scatterers provided by the top layers. Whereas, in single layer MoS_2, the scattering effect of ion gel is more prominent as the charge scatterers decrease the carrier mobility resulting in the four times reduction in drain current. However, similar to multilayer MoS_2, after the introduction of ion gel, the "off" current in

DOI: 10.1021/acsami.7b06071
ACS Appl. Mater. Interfaces 2017, 9, 26983−26989

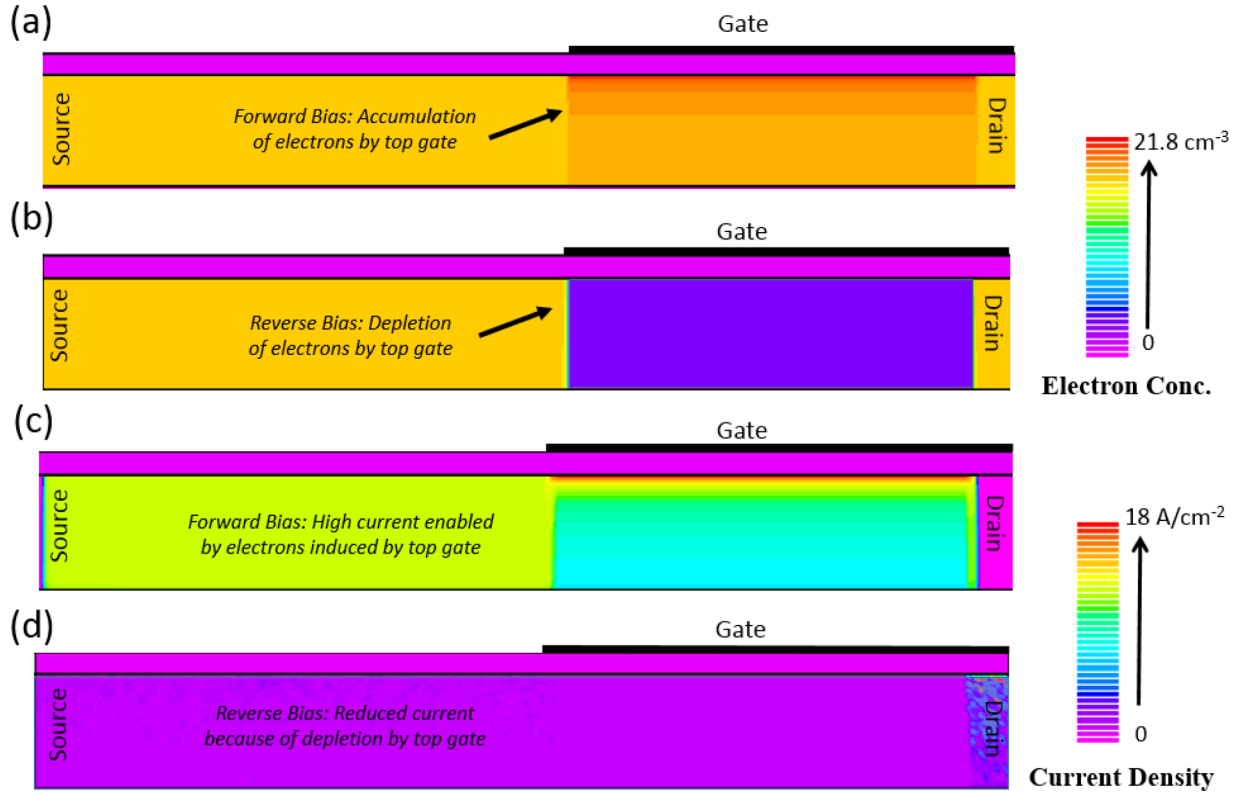

Figure 6. Silvaco TCAD simulation results showing (a and b) electrons concentration profile during forward and reverse bias, respectively and (c and d) electron current density profile during forward and reverse bias, respectively.

monolayer MoS_2 also increases from 90 pA (Figure 3b) to 1 nA (Figure 3d) at $V_g = -50$ V and $V_d = 1$ V. This increase in the "off" current can be similarly attributed to the induced electrons by ion gel near negative electrode as shown in inset of Figure 3d as well as GIDL. Since the band gap of single layer MoS_2 is higher (~1.8 eV) than multilayer MoS_2 (~1.2 eV), therefore, the GIDL is also less prominent in single layer MoS_2 and the value of "off" current in single layer MoS_2 is much less than few layer MoS_2. Near $V_g = -50$ V, in Figure 3d, the current after reaching a minimum value, starts to increase again. This increase in "off" current with increasing negative back gate voltage can be attributed to the contributions from both GIDL as well as leakage through SiO_2 at high electric field.

Further, we fabricated a device with configuration shown in Figure 4a to demonstrate an application of the biasing effect of ion gel by source and drain electrodes. In this device, one electrode was selectively covered with PMMA using e-beam lithography. In this configuration, the uncovered electrode can selectively bias the ion gel as the covered electrode is encapsulated with PMMA such that no electrical contact can be formed with the ion gel droplet. When open electrode is negative and covered electrode is positive, ion gel will also get negative bias and the channel will accumulate electrons induced by the positive electric field generated by the polarized ions from the ion gel as explained by schematic in Figure 5a. This ion gel induced positive electric field also reduce the Schottky barrier width at the metal-MoS_2 interface of the negative electrode as shown in Figure 5c.[23−25] As the major component of the injected electrons are injected via field assisted thermionic emission which exponentially depend upon the width of the Schottky barrier. Therefore, the reduced Schottky barrier width at the metal-MoS_2 interface of the negative electrode enhances the tunneling probability of the electrons across the barrier and results in a significant increase in the drain current. This increase in current is around 2 orders of magnitude compared to the pristine device as shown in Figure 4b and c.

When the polarity is reversed such that the open electrode is positive and the covered electrode is negative, the injection of electrons in this configuration will be from electrode covered by PMMA. This PMMA encapsulation which isolates the ion gel from the electrode such that it can no longer modulate the carrier density in the MoS_2 channel. Therefore, at the covered electrode, Schottky barrier remains same as in pristine device. Whereas, by the virtue of positive voltage at the uncovered electrode which bias the ion gel such that a negative electric field is generated by the polarized ions of the ion gel. This negative electric field will deplete the electrons from MoS_2 channel as shown in Figure 5b and results in a four times reduction of current as compared to pristine device.

Moreover, recent study shows that some charge transfer can also occur between organic polyelectrolyte and 2D materials.[26] Therefore, to reveal any charge transfer between ion gel and MoS_2, we performed the Raman spectroscopy of our monolayer MoS_2 device before and after the introduction of ion gel as shown in Figure S1. Raman spectroscopy can determine the charge transfer/doping in MoS_2: n-doping in MoS_2 results in decrease of peak frequency difference between A_{1g} and E_{2g} modes while p-doping cause relative shifting of the Raman active modes in opposite direction.[27] However, as shown in Figure S1, in our device, we did not observe any shift in peak positions indicating that there is no observable charge transfer between ion gel and MoS_2.

DOI: 10.1021/acsami.7b06071
ACS Appl. Mater. Interfaces 2017, 9, 26983−26989

These results are further verified by modeling an equivalent structure of ion gel self-biased diode in TCAD simulator "Atlas" of Silvaco. The primary focus of simulation results is on the modulation of carrier concentration (accumulation/depletion) and electric current density by the ion gel in MoS_2 device. The equivalent structure consists of a back gated MoS_2 FET, in which the effect of ion gel was simulated by the electric field of an extended electrode which is separated by 1 nm thick SiO_2 from the active channel, as shown in Figure S3. Although this arrangement cannot simulate the exact behavior of the effect of ion gel but can sufficiently mirror the electrostatics profile of the device and thus facilitate in the understanding of multiple bias effects by providing insight into the electrostatic and current density profile in such a device. As discussed in previous sections and shown in Figure 2c and 3c, the working of ion gel in self-biased configuration involves depletion of electrons when positive voltage is applied to the electrode and vice versa. Therefore, in simulations, the effect of ion gel is considered by applying an image voltage (opposite in polarity to main electrode voltage) to the extended electrode. When a negative voltage (−1.5 V) is applied to drain electrode and its image voltage (1.5 V) is applied to the top electrode, the carrier density in the region under the top electrode is increased up to 10^{21} cm^{-3} (Figure 6a). Similarly, the current density is also increased and the majority of current flows near top interface as shown in Figure 6c. Contrary to that, when the polarity is reversed such that, a positive voltage (1.5 V) is applied to drain electrode and its image negative voltage (−1.5 V) is applied to top electrode, it results in the depletion of the channel under the electrode and drastic reduction in the current density in the channel as shown in Figure 6b and d, respectively. These variations in the carrier concentration and current density with the polarity of the top electrode matches well with the observed experimental results and thus explains the asymmetry in $I-V_d$ curve of the self-biased diodes.

Finally, the observed diode-like characteristics in Figure 4c are also modeled with the Shockley diode equation as follows:[28,29]

$$|I_d| = |I_r|\left(\exp\left(\frac{qV_d}{nk_BT}\right) - 1\right) \quad (1)$$

$$I_r = AA^*T^2\exp\left(\frac{-q\phi_b}{k_BT}\right) \quad (2)$$

where I_d is the drain current, V_d is the applied voltage across junction, q is the electronic charge, n is the ideality factor, k_B is the Boltzmann constant, T is the temperature in Kelvin, I_r is the reverse saturation current, A is the area of the Schottky junction, A^* is the effective Richardson constant. The ideality factor, n, is derived from the slope of the $\ln\left(\frac{|I_d|}{|I_r|} + 1\right)$ versus V_d curve using the modified equation for large internal series resistance (R_s).[29]

$$|I_d| = |I_r|\left(\exp\left(\frac{q(V_d - I_dR_s)}{nk_BT}\right) - 1\right) \quad (3)$$

The best fit was obtained for resistance $R_s \approx 0.6$ MΩ and an ideality factor of 1.9 was obtained from the slope of the curve as shown in inset of Figure 4c. The higher value of ideality factor is possibly due to the high resistance of the MoS_2 layer and other nonideal factors like the intrinsic material defects in the MoS_2, process chemical residue and the interface states at the contacts that can account for the nonideal recombination processes resulting in the higher value of ideality factor.[28,30] Since the modulation of Schottky barrier width at the electrode which injects electrons will dictate the device current, therefore, we observe 10^2 times increase in current for one polarity but only four times reduction in current for opposite polarity.[31,32] A high rectification of around 10^3 is achieved by the self-biasing mechanism of ion gel and without using any conventional doping method. This diode behavior can find ready application in broad areas which require asymmetric transport for rectification purposes.

3. CONCLUSIONS

Self-biased diodes have been fabricated with a high asymmetry in output characteristics curve of around 10^3 and an ideality factor of 1.9. During forward bias, the reduction of Schottky barrier width by the electric field of self-biased ion gel enables an efficient injection of electrons by tunneling at metal-MoS_2 interface. Whereas, in reverse bias, depletion of electron in the channel by the electric field of self-biased ion gel reduces the device current. Finally, Silvaco TCAD simulations are carried out and the simulated results match well in principle with the experimental analysis.

4. EXPERIMENTAL SECTION

MoS_2 devices were prepared by exfoliating MoS_2 at a 285 nm thick SiO_2 layer on a heavily doped n-type Si substrate. The suitable flakes were selected by optical microscope and after that the source and drain contacts were defined by photolithography followed by Cr/Au (10/30 nm) deposition in electron-beam evaporation system and lift off in acetone. The ion gel solution was prepared by mixing the polymer PS-PMMA-PS and the ionic liquid EMIM-TFSI into an ethyl propionate solvent (weight ratio of polymer: ionic liquid: solvent = 0.7:9.3:20).[33] A 5 μL droplet of ionic liquid was dropped on the MoS_2 device in such a manner that the droplet covers the entire metal contacted region of the MoS_2 flake. To cover one electrode with PMMA, PMMA was spin coated at 4000 rpm, baked and then patterned by electron beam lithography.

■ ASSOCIATED CONTENT

Supporting Information

The Supporting Information is available free of charge on the ACS Publications website at DOI: 10.1021/acsami.7b06071.

Raman spectrum of single-layer device, leakage current profile of back gate and ion gel, device structure and parameters used for simulation, and electric field profile of device used for simulation (PDF)

■ AUTHOR INFORMATION

Corresponding Author

*E-mail: ghkim@skku.edu.

ORCID

Sun Jin Yun: 0000-0002-3665-0393

Gil-Ho Kim: 0000-0003-2479-5357

Notes

The authors declare no competing financial interest.

■ ACKNOWLEDGMENTS

This research was supported by Basic Science Research Program through the National Research Foundation of Korea (NRF) funded by the Ministry of Education, Science and

DOI: 10.1021/acsami.7b06071
ACS Appl. Mater. Interfaces 2017, 9, 26983−26989

Technology (2016R1A2A2A05921925), NRF-2016R1D1A1B03932455, and Korea Research Fellowship Program through the NRF funded by the Ministry of Science, ICT, and Future Planning (2015H1D3A1062519). This work was partly supported by Institute for Information & Communications Technology Promotion (IITP) grant funded by the Korea government (MSIP) (B0117-16-1003, Fundamental technologies of two-dimensional materials and devices for the platform of new-functional smart devices).

REFERENCES

(1) Wang, Q. H.; Kalantar-Zadeh, K.; Kis, A.; Coleman, J. N.; Strano, M. S. Electronics and Optoelectronics of Two-Dimensional Transition Metal Dichalcogenides. *Nat. Nanotechnol.* **2012**, *7* (11), 699−712.
(2) Xu, M.; Liang, T.; Shi, M.; Chen, H. Graphene-Like Two-Dimensional Materials. *Chem. Rev.* **2013**, *113* (5), 3766−3798.
(3) Chhowalla, M.; Shin, H. S.; Eda, G.; Li, L.-J.; Loh, K. P.; Zhang, H. The Chemistry of Two-Dimensional Layered Transition Metal Dichalcogenide Nanosheets. *Nat. Chem.* **2013**, *5* (4), 263−275.
(4) Das, S.; Chen, H.-Y.; Penumatcha, A. V.; Appenzeller, J. High Performance Multilayer MoS_2 Transistors with Scandium Contacts. *Nano Lett.* **2013**, *13* (1), 100−105.
(5) Ganatra, R.; Zhang, Q. Few-Layer MoS_2: A Promising Layered Semiconductor. *ACS Nano* **2014**, *8* (5), 4074−4099.
(6) Yoon, Y.; Ganapathi, K.; Salahuddin, S. How Good Can Monolayer MoS_2 Transistors Be? *Nano Lett.* **2011**, *11* (9), 3768−3773.
(7) Kim, S. H.; Hong, K.; Xie, W.; Lee, K. H.; Zhang, S.; Lodge, T. P.; Frisbie, C. D. Electrolyte-Gated Transistors for Organic and Printed Electronics. *Adv. Mater.* **2013**, *25* (13), 1822−1846.
(8) Lee, J.; Kaake, L. G.; Cho, J. H.; Zhu, X.-Y.; Lodge, T. P.; Frisbie, C. D. Ion Gel-Gated Polymer Thin-film Transistors: Operating Mechanism and Characterization of Gate Dielectric Capacitance, Switching Speed, and Stability. *J. Phys. Chem. C* **2009**, *113* (20), 8972−8981.
(9) Pu, J.; Yomogida, Y.; Liu, K.-K.; Li, L.-J.; Iwasa, Y.; Takenobu, T. Highly Flexible MoS_2 Thin-film Transistors with Ion Gel Dielectrics. *Nano Lett.* **2012**, *12* (8), 4013−4017.
(10) Perera, M. M.; Lin, M.-W.; Chuang, H.-J.; Chamlagain, B. P.; Wang, C.; Tan, X.; Cheng, M. M.-C.; Tománek, D.; Zhou, Z. Improved Carrier Mobility in Few-Layer MoS_2 Field-Effect Transistors with Ionic-Liquid Gating. *ACS Nano* **2013**, *7* (5), 4449−4458.
(11) de Mello, J. C.; Tessler, N.; Graham, S.; Friend, R. Ionic Space-Charge Effects in Polymer Light-Emitting Diodes. *Phys. Rev. B: Condens. Matter Mater. Phys.* **1998**, *57* (20), 12951.
(12) Zhang, Y.; Ye, J.; Matsuhashi, Y.; Iwasa, Y. Ambipolar MoS_2 Thin Flake Transistors. *Nano Lett.* **2012**, *12* (3), 1136−1140.
(13) Ye, J.; Zhang, Y.; Akashi, R.; Bahramy, M.; Arita, R.; Iwasa, Y. Superconducting Dome in a Gate-Tuned Band Insulator. *Science* **2012**, *338* (6111), 1193−1196.
(14) Braga, D.; Gutiérrez Lezama, I.; Berger, H.; Morpurgo, A. F. Quantitative Determination of the Band Gap of WS_2 with Ambipolar Ionic Liquid-Gated Transistors. *Nano Lett.* **2012**, *12* (10), 5218−5223.
(15) Kim, B. J.; Jang, H.; Lee, S.-K.; Hong, B. H.; Ahn, J.-H.; Cho, J. H. High-Performance Flexible Graphene Field Effect Transistors with Ion Gel Gate Dielectrics. *Nano Lett.* **2010**, *10* (9), 3464−3466.
(16) Allain, A.; Kis, A. Electron and Hole Mobilities in Single-Layer WSe_2. *ACS Nano* **2014**, *8* (7), 7180−7185.
(17) Pei, T.; Bao, L.; Wang, G.; Ma, R.; Yang, H.; Li, J.; Gu, C.; Pantelides, S.; Du, S.; Gao, H.-j. Few-Layer SnSe2 Transistors with High On/Off Ratios. *Appl. Phys. Lett.* **2016**, *108* (5), 053506.
(18) Zhang, Y.; Ye, J.; Yomogida, Y.; Takenobu, T.; Iwasa, Y. Formation of a Stable p−n Junction in a Liquid-Gated MoS_2 Ambipolar Transistor. *Nano Lett.* **2013**, *13* (7), 3023−3028.
(19) Asenov, A.; Brown, A. R.; Davies, J. H.; Kaya, S.; Slavcheva, G. Simulation of Intrinsic Parameter Fluctuations in Decananometer and Nanometer-Scale MOSFETs. *IEEE Trans. Electron Devices* **2003**, *50* (9), 1837−1852.
(20) Bernstein, K.; Frank, D. J.; Gattiker, A. E.; Haensch, W.; Ji, B. L.; Nassif, S. R.; Nowak, E. J.; Pearson, D. J.; Rohrer, N. J. High-Performance CMOS Variability in the 65-nm Regime and Beyond. *IBM J. Res. Dev.* **2006**, *50* (4.5), 433−449.
(21) Lee, C.; Yan, H.; Brus, L. E.; Heinz, T. F.; Hone, J.; Ryu, S. Anomalous Lattice Vibrations of Single-and Few-Layer MoS_2. *ACS Nano* **2010**, *4* (5), 2695−2700.
(22) Das, S.; Appenzeller, J. Where Does the Current Flow in Two-Dimensional Layered Systems? *Nano Lett.* **2013**, *13* (7), 3396−3402.
(23) Yang, L.; Majumdar, K.; Du, Y.; Liu, H.; Wu, H.; Hatzistergos, M.; Hung, P.; Tieckelmann, R.; Tsai, W.; Hobbs, C.; Ye, P. D. High-Performance MoS_2 Field-Effect Transistors Enabled by Chloride Doping: Record Low Contact Resistance (0.5 kΩ· μm) and Record High Drain Current (460 μA/μm). *Symp. VLSI Technol., Dig. Technol. Pap.* **2014**, 1−2.
(24) Yang, L.; Majumdar, K.; Liu, H.; Du, Y.; Wu, H.; Hatzistergos, M.; Hung, P.; Tieckelmann, R.; Tsai, W.; Hobbs, C.; et al. Chloride Molecular Doping Technique on 2D Materials: WS2 and MoS_2. *Nano Lett.* **2014**, *14* (11), 6275−6280.
(25) Ahmed, F.; Choi, M. S.; Liu, X.; Yoo, W. J. Carrier Transport at the Metal−MoS_2 Interface. *Nanoscale* **2015**, *7* (20), 9222−9228.
(26) Brus, V. V.; Gluba, M. A.; Mai, C. K.; Fronk, S. L.; Rappich, J.; Nickel, N. H.; Bazan, G. C. Nanocomposites: Conjugated Polyelectrolyte/Graphene Hetero-Bilayer Nanocomposites Exhibit Temperature Switchable Type of Conductivity. *Adv. Electron. Mater.* **2017**, *3*, 1600515.
(27) Shi, Y.; Huang, J.-K.; Jin, L.; Hsu, Y.-T.; Yu, S. F.; Li, L.-J.; Yang, H. Y. Selective Decoration of Au Nanoparticles on Monolayer MoS_2 Single Crystals. *Sci. Rep.* **2013**, *3*, 1839.
(28) Jariwala, D.; Sangwan, V. K.; Wu, C.-C.; Prabhumirashi, P. L.; Geier, M. L.; Marks, T. J.; Lauhon, L. J.; Hersam, M. C. Gate-Tunable Carbon Nanotube−MoS_2 Heterojunction pn Diode. *Proc. Natl. Acad. Sci. U. S. A.* **2013**, *110* (45), 18076−18080.
(29) Sutar, S.; Agnihotri, P.; Comfort, E.; Taniguchi, T.; Watanabe, K.; Ung Lee, J. Reconfigurable pn Junction Diodes and the Photovoltaic Effect in Exfoliated MoS_2 Films. *Appl. Phys. Lett.* **2014**, *104* (12), 122104.
(30) Mak, K. F.; He, K.; Lee, C.; Lee, G. H.; Hone, J.; Heinz, T. F.; Shan, J. Tightly Bound Trions in Monolayer MoS_2. *Nat. Mater.* **2013**, *12* (3), 207−211.
(31) Choi, Y.; Kang, J.; Jariwala, D.; Kang, M. S.; Marks, T. J.; Hersam, M. C.; Cho, J. H. Low-Voltage Complementary Electronics from Ion-Gel-Gated Vertical Van der Waals Heterostructures. *Adv. Mater.* **2016**, *28* (19), 3742−3748.
(32) Khan, M. A.; Rathi, S.; Lee, I.; Li, L.; Lim, D.; Kang, M.; Kim, G.-H. P-doping and Efficient Carrier Injection Induced by Graphene Oxide for High Performing WSe_2 Rectification Devices. *Appl. Phys. Lett.* **2016**, *108* (9), 093104.
(33) Chu, L.; Schmidt, H.; Pu, J.; Wang, S.; Ozyilmaz, B.; Takenobu, T.; Eda, G. Charge Transport in Ion-Gated Mono-, Bi-, and Trilayer MoS_2 Field Effect Transistors. *Sci. Rep.* **2015**, *4*, 7293.

DOI: 10.1021/acsami.7b06071
ACS Appl. Mater. Interfaces 2017, 9, 26983−26989